nature neuroscience

Astrocytes contain a vesicular compartment that is competent for regulated exocytosis of glutamate

Paola Bezzi[1,2,6], Vidar Gundersen[1,3,6], José Luis Galbete[1], Gerald Seifert[4], Christian Steinhäuser[4], Ethel Pilati[1] & Andrea Volterra[1,2,5]

Astrocytes establish rapid cell-to-cell communication through the release of chemical transmitters. The underlying mechanisms and functional significance of this release are, however, not well understood. Here we identify an astrocytic vesicular compartment that is competent for glutamate exocytosis. Using postembedding immunogold labeling of the rat hippocampus, we show that vesicular glutamate transporters (VGLUT1/2) and the vesicular SNARE protein, cellubrevin, are both expressed in small vesicular organelles that resemble synaptic vesicles of glutamatergic terminals. Astrocytic vesicles, which are not as densely packed as their neuronal counterparts, can be observed in small groups at sites adjacent to neuronal structures bearing glutamate receptors. Fluorescently tagged VGLUT-containing vesicles were studied dynamically in living astrocytes by total internal reflection fluorescence (TIRF) microscopy. After activation of metabotropic glutamate receptors, astrocytic vesicles underwent rapid (milliseconds) Ca^{2+}- and SNARE-dependent exocytic fusion that was accompanied by glutamate release. These data document the existence of a Ca^{2+}-dependent quantal glutamate release activity in glia that was previously considered to be specific to synapses.

Astrocytes release a variety of chemical mediators by which they respond and signal to their environment (for review, see ref. 1). The underlying mechanisms for this release remain largely undefined. One way in which astrocytes initiate intercellular communication is by elevation of their internal Ca^{2+} concentration ($[Ca^{2+}]_i$). This event may depend on either an intrinsic oscillatory activity[2] or on the stimulation of astrocyte surface receptors, for example by neurotransmitters released during synaptic activity[3–5] or by gliotransmitters involved in long-range signal propagation[6,7]. The best-characterized consequence of such $[Ca^{2+}]_i$ elevations is the release of glutamate[8,9], by which astrocytes modulate neuronal excitability and synaptic functions (for review, see ref. 10). Regulated exocytosis could be the process that sustains this form of glutamate release, in view of its (i) Ca^{2+} dependency, (ii) sensitivity to toxins that are highly specific for blocking exocytosis from neurosecretory cells[9,11–13] and (iii) capacity to generate quantal-like current responses in glutamate-sniffing cells[13]. In further support of this hypothesis, astrocytes express secretion-associated proteins and contain secretion-associated organelles (for review, see ref. 14). Despite the above indications, the evidence for an exocytic process is largely indirect and stems almost exclusively from studies in cultured astrocytes. Indeed, no study to date has been able to show the presence of a vesicular compartment that is competent for glutamate exocytosis in tissue astrocytes *in situ*. Lack of direct evidence has given rise to debate and brought some investigators to question the notion that astrocytes release glutamate by exocytosis *in situ*[15].

Here we have taken experimental approaches that permit us to address the above issue directly. The elusive glutamate-containing vesicles were sought in tissue astrocytes by postembedding immunogold electron microscopy using as specific markers the members of the vesicular glutamate transporter (VGLUT) family[16] in combination with markers of the vesicle fusion core complex, the v-SNAREs[17]. To visualize glutamate exocytosis directly and to generate information about its kinetics, glutamatergic vesicles were tagged in living astrocytes with a VGLUT–enhanced green fluorescent protein (EGFP) construct, loaded with a fluorescent marker of exocytosis[18] and studied dynamically[19,20] with TIRF imaging[21]. By focusing on cellular events occurring within tens to hundreds of nanometers from the plasma membrane, TIRF imaging is ideally suited to study the dynamics of exocytosis with high temporal resolution at the level of individual vesicles[22].

Our study shows the presence in astrocytes of a vesicular compartment involved in the uptake and regulated exocytosis of glutamate and provides the first description of its ultrastructural and functional properties.

RESULTS

Hippocampal astrocytes contain VGLUT-positive microvesicles

If, in astrocytes, Ca^{2+}-regulated glutamate release[8,9] takes place by exocytosis, these cells must contain a glutamate-storing and -releasing vesicular compartment. We initially investigated whether

[1]Department of Cell Biology and Morphology, University of Lausanne, and [2]Cellular Imaging Facility UNIL-CHUV-Technological Development Unit, Rue du Bugnon 9, 1005 Lausanne, Switzerland. [3]Anomical Institute and Centre for Molecular Biology and Neuroscience, University of Oslo, POB 1105 Blindern, 0317 Oslo, Norway. [4]Department of Experimental Neurobiology, Neurosurgery, University of Bonn, Sigmund-Freud-Str. 25, D-53105 Bonn, Germany. [5]Department of Pharmacological Sciences and Center of Excellence on Neurodegenerative Diseases, University of Milan, Via Balzaretti 9, Milan 20133, Italy. [6]These authors contributed equally to this work. Correspondence should be addressed to A.V. (Andrea.Volterra@ibcm.unil.ch).

Published online 23 May 2004; doi:10.1038/nn1246

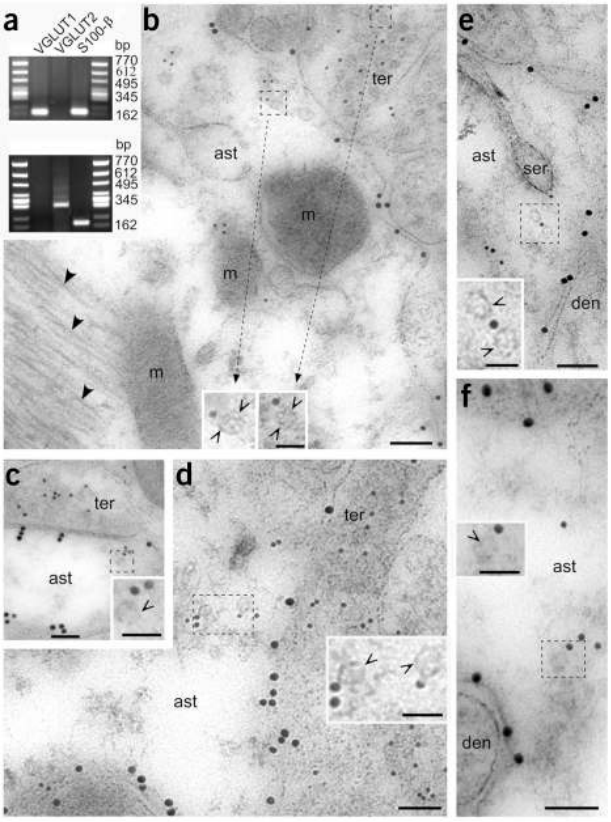

Figure 1 VGLUT-positive small vesicular organelles in astrocytic processes that face neuronal structures in the hippocampus. (**a**) cDNA gels from electrophysiologically identified astrocytes of the outer molecular layer of the hippocampal dentate gyrus show the coexpression of the astrocyte marker S100β (175 bp) and VGLUT1 (165 bp, upper gel) or VGLUT2 (286 bp, lower gel). (**b**–**f**) Electron micrographs of (**b**–**e**) VGLUT1 and (**f**) VGLUT2 (small gold particles) in astrocyte processes in the molecular layers of the dentate gyrus. The astrocyte processes are identified by labeling for GLT/GLAST[25] (large gold particles) and by the presence of filaments (filled arrowheads). In **b**, VGLUT1 is located in small groups over vesicular organelles in an astrocyte process (ast) close to the plasma membrane facing a VGLUT1-positive nerve terminal (ter). Insets: Higher magnifications highlighting the similar appearance of VGLUT1-positive vesicles in astrocytes and in nerve terminals (open arrowheads). m, mitochondria. Other examples of VGLUT1-positive vesicles are shown in **c** and **d**, just beneath the plasma membrane that opposes VGLUT1-positive nerve terminals (ter). Insets: Higher magnifications showing the astrocyte vesicles (open arrowheads) labeled for VGLUT1. In **e**, VGLUT1-positive vesicular organelles are close to a tubular structure resembling smooth endoplasmatic reticulum (ser). Inset: Higher magnification showing a VGLUT1 gold particle belonging to either of the vesicles (open arrowheads). den, dendrite. (**f**) VGLUT2 labeling in an astrocyte process. Inset: A vesicular organelle (open arrowhead) is positive for VGLUT2. den, dendrite. Scale bars, 100 nm in **b**–**f** and 50 nm in insets.

astrocytes *in situ* express VGLUTs, the proteins responsible for taking up glutamate into synaptic vesicles in glutamatergic neurons, by focusing on the VGLUT1 and VGLUT2 isoforms[16]. We whole-cell patch clamped cells of the molecular layer of the dentate gyrus from rat (postnatal day (P) 35–70) hippocampal slices. Those displaying electrophysiological properties typical of 'passive' astrocytes[23] were then subjected to multiplex single-cell polymerase chain reaction after reverse transcription of RNA (RT-PCR)[24]. Of the 37 cells analyzed, 34 expressed the mRNA for S100β, a typical astrocyte marker, confirming their astrocytic nature. In almost 25% of such cells, we detected VGLUT transcripts, notably VGLUT1 in seven cells and VGLUT2 in one cell (**Fig. 1a**). Similar proportions were observed by confocal immunofluorescence microscopy of the dentate molecular layers, using glial fibrillary acidic protein (GFAP) as an astrocyte marker (32% of GFAP-labeled cells were positive for VGLUT1 and 8% for VGLUT2). To determine the ultrastructural localization of VGLUT1 and VGLUT2 in astrocytes, we carried out immunogold cytochemistry in astrocyte processes in the dentate gyrus. The processes were recognized by the presence of filaments and/or by labeling for the astrocyte plasma membrane glutamate transporters, GLT and GLAST[25]. Indeed, such processes showed immunogold

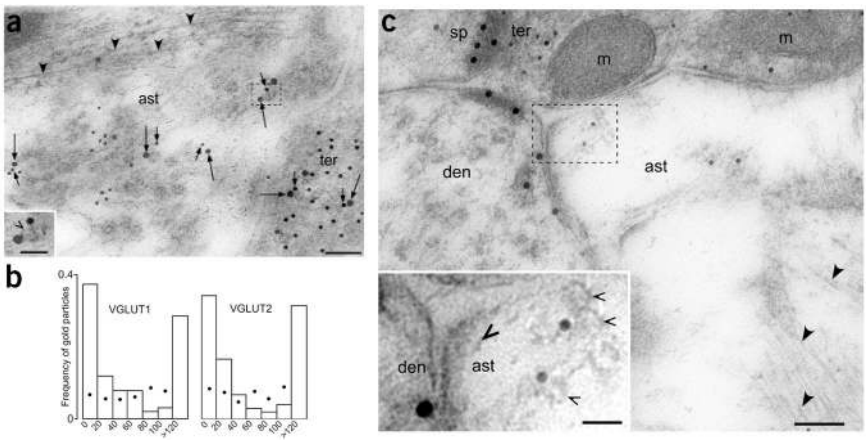

Figure 2 Colocalization of VGLUTs and cellubrevin in astrocytic vesicles: proximity to neuronal membranes carrying NMDA receptors. (**a**) VGLUT1 (small gold particles; short arrows) and cellubrevin (large gold particles; long arrows) localize to small vesicular organelles in an astrocyte process (ast) containing filaments (filled arrowheads). The astrocyte process is close to a nerve terminal (ter) that expresses VGLUT1 and cellubrevin on synaptic vesicles. Inset: Higher magnifications showing association of VGLUT1 and cellubrevin with the same vesicle (open arrowhead). (**b**) Analysis of the distance from the center of each VGLUT1 or VGLUT2 gold particle to the center of the closest cellubrevin gold particle in astrocyte processes (see **a**). The distribution of VGLUT1 or VGLUT2 versus cellubrevin intercenter distances, sorted into bins of 20 nm, indicates a close spatial relationship and is significantly different from that of VGLUT1 or VGLUT2 versus random points (filled circles; $P < 0.001$, chi-squared test). (**c**) Double immunogold labeling for VGLUT1 (small gold particles) and NMDA receptors (large gold particles). Note VGLUT1 vesicles in an astrocyte process (ast) containing filaments (filled arrowheads). The astrocyte plasma membrane is close to NMDA receptors located in the postsynaptic density of two synapses made by a VGLUT1-containing terminal (ter) and in the extrasynaptic dendritic membrane. Inset: Higher magnification showing the short distance between the astrocyte VGLUT1 vesicles (open arrowheads) and the extrasynaptic NMDA receptors. Note the vesicle (large open arrowhead) nearly attached to the astrocyte plasma membrane. Scale bars, 100 nm in **a** and **c** and 50 nm in insets.

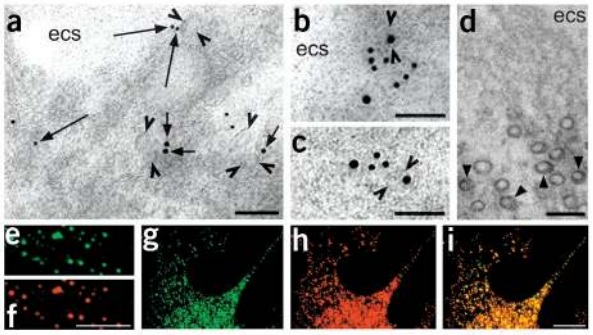

Figure 3 Colocalization of VGLUTs and cellubrevin in small vesicles in the processes of cultured astrocytes. (**a**) Electron micrograph showing immunogold localization of VGLUT1 (small gold particles; long arrows) and VGLUT2 (large gold particles; short arrows) on small vesicular organelles (open arrowheads) in a process of a cultured astrocyte. Note the vicinity of some of these organelles to the surface of the process. ecs, extracellular space. (**b**,**c**) Immunogold colocalization of VGLUT1 (small gold particles in **b**) or VGLUT2 (small gold particles in **c**) and cellubrevin (large gold particles) on the same vesicular organelles (open arrowheads) in a process of a cultured astrocyte. (**d**) Visualization of discrete small vesicles immunolabeled for EGFP in a process of a cultured astrocyte transfected with a cellubrevin-EGFP construct. Note that vesicular organelles highlighted by the peroxidase product (filled arrowheads) are similar in size and shape to those that are immunogold labeled for VGLUT1 and VGLUT2 in **a**–**c**. ecs, extracellular space. Bars in **a**–**d**, 100 nm. (**e**–**f**) EGFP fluorescence (green in **e**) in a process of an astrocyte that was transfected as in **d** localizes with immunofluorescent labeling for endogenous VGLUT2 (red in **f**). Bar, 10 μm. (**g**–**i**) Images from an astrocyte transfected with the VGLUT2-EGFP construct. The punctate EGFP signal (green in **g**) and the immunofluorescent signal for endogenous cellubrevin (red in **h**) largely colocalize (yellow in **i**). Scale bar, 10 μm.

signals for both VGLUT1 (**Fig. 1b–e**) and VGLUT2 (**Fig. 1f**). In particular, signals for VGLUT1 were observed in about 27% of the astrocytic processes, and signals for VGLUT2 were seen in about 8%. The densities of VGLUT1 and VGLUT2 immunogold particles in the astrocyte processes, although lower than those in nerve terminals (by about sevenfold and eightfold, respectively), were significantly higher than those in postsynaptic dendrites (by threefold and fourfold) as well as in mitochondria (by sevenfold and fourfold; $P < 0.01$, two-tailed Mann-Whitney U-test).

In the astrocyte processes, gold particles that indicated the presence of VGLUT1 and VGLUT2 were associated with small vesicular organelles, which were often present in small groups close to the plasma membrane that is in opposition to neuronal structures (**Fig. 1b–f**). The shape and size of the VGLUT-containing vesicles (mean diameter, 27.6 ± 12.3 nm; $n = 49$) were similar to those of the synaptic vesicles of VGLUT-positive nerve terminals (mean diameter, 26.9 ± 8.6 nm; $n = 45$; **Fig. 1b**).

To investigate whether these astrocytic organelles are homologous to synaptic vesicles, double-labeling immunogold experiments were carried out with antibodies to VGLUT1 or VGLUT2 and to vesicle-associated membrane protein 2 (VAMP2) or cellubrevin. The latter two proteins (which are both v-SNAREs) are expressed in cultured astrocytes[14]. We could not detect significant VAMP2 labeling in the astrocytic processes, whereas nerve terminals were clearly labeled (data not shown). In contrast, cellubrevin was expressed in small astrocytic vesicular organelles similar to those expressing VGLUT1 and VGLUT2 (mean diameter, 29.1 ± 12.8 nm; $n = 20$), as well as in synaptic vesicles of nerve terminals (**Fig. 2a**).

To investigate whether the astrocytic vesicles that were positive for VGLUT1 or VGLUT2 coincide with those that are positive for cellubrevin, we analyzed the distance between the center of VGLUT1- or VGLUT2-associated gold particles and the center of the nearest cellubrevin-associated gold particle. The distributions of the minimum distances were similar for VGLUT1 and VGLUT2, with the highest relative numbers of VGLUT gold particles being closer than 20 nm to the nearest cellubrevin gold particle (**Fig. 2b**).

Because of the diameter of the vesicles (~30 nm) and the lateral resolution of the immunogold method (~40 nm; ref. 25), VGLUT and cellubrevin gold particles that were separated by up to 110 nm could still denote epitopes in the same vesicle membrane. Most VGLUT and cellubrevin gold particles were located within this distance. Moreover, the VGLUT1– and VGLUT2–cellubrevin distributions were significantly different from the distribution of distances between VGLUT1

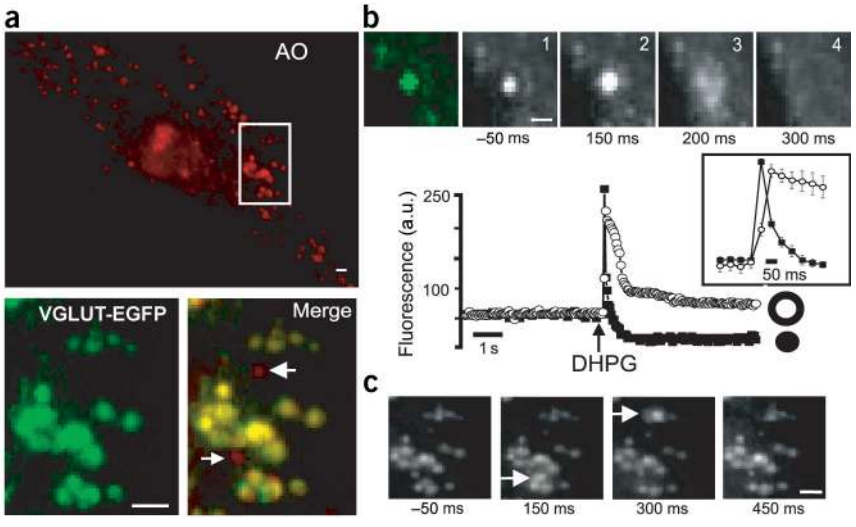

Figure 4 Exocytic fusions of VGLUT-positive vesicles monitored in living astrocytes. (**a**) Astrocyte vesicular organelles doubly fluorescent for acridine orange (AO) and VGLUT-EGFP. The evanescent microscopic image shows acridine orange fluorescence (red); the lower panels, a higher magnification of the boxed region in the red image, show EGFP fluorescence (green) and overlap of acridine orange and EGFP fluorescence (yellow). Arrows indicate acridine orange–filled organelles (red) that do not correspond to VGLUT+ vesicles. (**b**) Acridine orange flashes signaling vesicle fusions. Top, sequential images (1 to 4) of a single dye-loaded VGLUT+ vesicle fusing with the plasma membrane. The green image on the left confirms expression of VGLUT-EGFP. Times represent milliseconds before and during perfusion of 100 μM DHPG. Note increase in brightness (2), diffusion of dye (3) and disappearance of spot (4). Bottom, kinetics of fluorescence intensity changes (in arbitrary units) for the above spot, measured in a small circle enclosing the spot (filled squares) and in a concentric annulus around the circle (open circles). In the box are average kinetics of 10 flashes on a faster time scale. (**c**) Sequential images (left to right) showing two individual fusion events (arrows) occurring in the group of vesicles boxed in **a**. Scale bars, 1 μm in **a** and **b** and 2 μm in **c**.

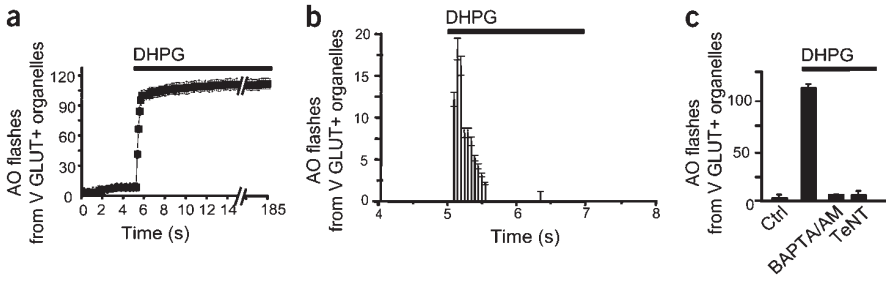

Figure 5 Properties of mGluR-evoked exocytosis of VGLUT+ vesicles. (**a**,**b**) DHPG (100 μM) elicits an exocytic burst. In **a**, the cumulative numbers of acridine orange flashes (corresponding to fusion events) are plotted against time during a 3-min application of DHPG ($n = 10$). In **b**, the time distribution of fusion events before, during and after a 2-s pulse of DHPG are shown. Each histogram indicates the number of flashes counted in a 50-ms frame ($n = 9$). (**c**) Ca^{2+} and VAMP/cellubrevin dependency of DHPG-evoked vesicle fusions. Acridine orange flashes in response to 100 μM DHPG are reduced to control (Ctrl) levels if cells are preincubated with either BAPTA-AM (50 μM, 30 min; $n = 5$) or TeNT (10 μg/ml, 8 h; $n = 5$). TeNT-treated astrocytes respond to DHPG with $[Ca^{2+}]_i$ elevations that are similar to those seen in untreated cells (data not shown).

or VGLUT2 immunogold particles and that of points randomly distributed over the astrocyte (**Fig. 2b**). These data strongly support the localization of VGLUT1 and VGLUT2 in cellubrevin-containing vesicles (**Fig. 2a**).

To explore the possible functional relevance of astrocytic VGLUT-positive vesicles near neuronal terminals (**Figs. 1b–d** and **2a**,**c**) or dendrites (**Figs. 1e**,**f** and **2c**), we carried out double-labeling immunogold experiments for VGLUT1 and NMDA (*N*-methyl-D-aspartate) receptors. We could find groups of astrocytic VGLUT-containing vesicles that were opposite extrasynaptic dendritic membranes carrying NMDA receptors and were in close proximity to NMDA receptor–positive synapses (**Fig. 2c**). Astrocytic VGLUT-carrying vesicles facing presynaptically expressed NMDA receptors were also observed.

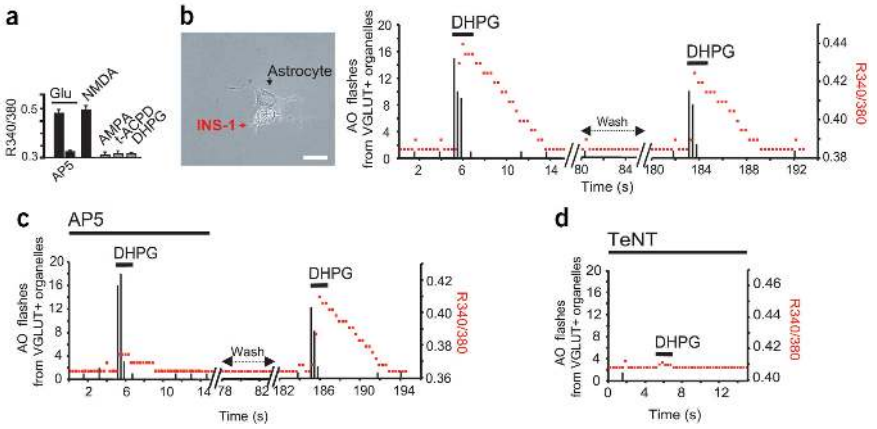

Figure 6 Astrocyte vesicle fusions evoke glutamate-dependent $[Ca^{2+}]_i$ elevations in INS-1 cells. (**a**) INS-1 cells as glutamate-sniffing cells. Fura-2-loaded INS-1 cells show $[Ca^{2+}]_i$ elevation (R340/380) in response to glutamate (Glu, 100 μM; $n = 25$), which is inhibited by the NMDA receptor antagonist AP5 (50 μM; $n = 5$). They show a similar increase in response to NMDA (50 μM; $n = 4$), but not to AMPA (50 μM; $n = 7$) or mGluR agonists t-ACPD or DHPG (both 100 μM; $n = 6$ and 52, respectively). (**b**) On the left, an isolated cell pair formed by an astrocyte and an attached INS-1 cell. Scale bar, 20 μm. On the right, acridine orange flashes (black histograms) in the astrocyte and $[Ca^{2+}]_i$ changes (red trace) in the INS-1 cell were monitored in parallel (10 interlaced frames/s). Cells were challenged with two applications of DHPG (50 μM, 2 s) separated by a 3-min washing period (in the trace, 5 s of Wash). (**c**) $[Ca^{2+}]_i$ elevation in the INS-1 cell is glutamate dependent. Experiment as in **b** but in the presence of the NMDA receptor antagonist AP5 (100 μM; $n = 5$). $[Ca^{2+}]_i$ elevation in the INS-1 cell is blocked, whereas acridine orange flashes in the astrocyte are not; the inhibitory effect of AP5 is reversible upon washout. (**d**) Blocking exocytosis with TeNT (10 μg/ml, 8 h; $n = 4$) abolishes both acridine orange flashes in the astrocyte and $[Ca^{2+}]_i$ elevation in the INS-1 cell.

Regulated exocytosis of astrocytic VGLUT-carrying vesicles

To determine whether astrocytes release glutamate by regulated exocytosis of the VGLUT1-positive or VGLUT2-positive vesicular organelles, we studied astrocytes in culture. We first verified whether the vesicular system expressing VGLUTs in cultured astrocytes has properties analogous to those of the astrocytes in the dentate gyrus *in situ*. We found that VGLUT1-positive and/or VGLUT2-positive vesicular organelles (i) were present throughout the cultured astrocytes, including in the processes (**Fig. 3a**); (ii) had a diameter similar to vesicles in astrocytes *in situ* (**Fig. 3a–c**) and (iii) were immunopositive for cellubrevin (**Fig. 3b**,**c**; and negative for VAMP2, despite the presence of VAMP2 in the cultured cells), as indicated by a distribution analysis that was done as for the astrocytes *in situ*. The vesicular organelles could be distinctly visualized by transfecting astrocytes with a cellubrevin-EGFP construct (in which the tag is in the intraluminal portion of cellubrevin[26]) and by immunoperoxidase labeling of the astrocytes with antibodies to EGFP. This approach showed groups of discrete vesicles (**Fig. 3d**) that were similar in shape and size to those immunolabeled for VGLUTs (**Figs. 1b–f** and **2a** and **3a–c**). Immunofluorescence microscopy analysis confirmed coexpression of cellubrevin and VGLUTs (85 ± 7%, $n = 222$ vesicles; **Fig. 3e**,**f**).

The dynamics of VGLUT-positive vesicles were monitored in living astrocytes transfected with constructs of chimeric VGLUT1-EGFP or VGLUT2-EGFP fluorescent proteins. Either construct produced a punctate pattern of EGFP fluorescence that was widespread in the astrocytic cell soma and processes (**Fig. 3g**). Cellubrevin largely localized with VGLUT-EGFP dots (91 ± 5%, $n = 304$ vesicles; **Fig. 3h**,**i**), indicating that the organelle population that was labeled by the tagged transporters essentially corresponds to that carrying the endogenous transporters.

To establish whether VGLUT-EGFP-positive (VGLUT+) vesicles undergo regulated exocytosis, vesicles were stained with acridine orange, a dye that accumulates in a self-quenched state inside acidic compartments[18,19,27]. When an acridine orange–filled organelle fuses with the plasma membrane, the dye is released to the extracellular medium with the production of a 'flash', a localized and transient increase in fluorescent light, followed by a lateral spread of fluorescence (due to diffusion of the dye) and finally by the disappearance of the labeled organelle[19,20]. The dynamics of VGLUT+ vesicles lying just beneath the plasma mem-

brane[22] were followed in real time with TIRF imaging that was set to detect both acridine orange and EGFP fluorescence[18]. Typical TIRF images are shown (**Fig. 4a**). Acridine orange–positive organelles, which were frequently arranged in small groups, generally localized with VGLUT+ dots (76.8 ± 14%, $n = 40$ cells; **Fig. 4a**). Under resting conditions, these double-positive organelles showed slow Brownian motion (average displacement, 0.073 ± 0.011 μm/s; $n = 20$ cells). To assess whether this population of doubly fluorescent vesicles undergoes regulated exocytosis, we challenged astrocytes with α-latrotoxin (LTx), a direct stimulant of exocytosis[28]; the Ca^{2+} ionophore ionomycin (IONO) or dihydroxyphenylglicine (DHPG), an agonist of group I metabotropic glutamate receptors (mGluRs), which is known to evoke Ca^{2+}-dependent glutamate release in astrocytes[9,29]. All three agents induced acridine orange flashes, albeit with different efficacy and kinetics. (For results with LTx and IONO, see **Supplementary Fig. 1** and **Supplementary Note** online.) The time sequences of acridine orange fluorescence images (**Fig. 4b,c**) document fusion of individual VGLUT+ vesicles to the plasma membrane in response to DHPG. By plotting fluorescence against time in a small circle around acridine orange spots and in a concentric annulus around the circle[20], we consistently found that fluorescence initially increased in the circle, then spread into the annulus and finally declined, which is in line with what is expected for an exocytic event[20] (**Fig. 4b**). We counted the number of flashes per astrocyte (mean surface area, 1,165 ± 220 μm^2) observed during 3-min-long applications of DHPG. With 10, 100 and 1,000 μM DHPG, the number of flashes were 34 ± 5 ($n = 4$), 106 ± 12 ($n = 10$) and 120 ± 18 ($n = 6$), respectively. In contrast, buffer induced 10 ± 3 flashes/astrocyte ($n = 6$). Therefore, acridine orange flashes are a specific response to DHPG. Two features of this phenomenon are worth noting. First, only a fraction of the VGLUT+ vesicles in the TIRF field underwent a flash in response to DHPG (34 ± 10% with 1,000 μM DHPG). Second, the fusion events took place only at the very beginning of DHPG perfusion (**Fig. 5a**).

To better define the kinetics of exocytosis, we next applied DHPG in a 2-s pulse by electrovalve-driven microperfusion while acquiring acridine orange images at 20 interlaced frames/s (**Fig. 5b**; $n = 9$). DHPG-evoked exocytosis occurred in a single burst: the fusion rate (flashes/s) was low in the 2 s preceding application of the agent (0.5 ± 0.07) but abruptly increased by about 500-fold within 100–150 ms after the start of DHPG perfusion. The rate peaked in the next 50 ms (360 ± 22) and then declined to prestimulus values after a total of 600 ms, remaining constant during the rest of the DHPG application and in the poststimulus period. Further insight into the mGluR-evoked exocytic process was obtained by examining vesicle fate in VGLUT-EGFP images. At 300 ms after undergoing an acridine orange flash, vesicles monitored as EGFP spots showed two distinct fates: 40 ± 11% had disappeared, whereas 60 ± 2% persisted in place, without any significant change of fluorescence intensity ($n = 9$ cells).

Finally, the acridine orange flashes in response to DHPG were abolished by (i) preloading the cells with BAPTA/AM, which buffers $[Ca^{2+}]_i$ and prevents its increase after receptor activation (–88 ± 6%; **Fig. 5c**) or (ii) pre-exposing the cells to tetanus neurotoxin (TeNT), which cleaves both VAMP2 and cellubrevin, blocking vesicle fusion at the level of SNARE complex formation[30] (–95 ± 10%). The same treatments also abolish mGluR-dependent glutamate release[9,29], strongly indicating that flashes from VGLUT+ vesicles may represent exocytic fusions of glutamate-containing vesicles.

Exocytosis is accompanied by glutamate release

To show directly that fusions of VGLUT-positive vesicles correspond to glutamate release events, we plated astrocytes together with 'glutamate-sniffing' insulinoma-1 (INS-1) cells. Initial fura-2 experiments showed that, in the absence of astrocytes, INS-1 cells responded to local application of glutamate with rapid $[Ca^{2+}]_i$ elevation, which was inhibited by the NMDA receptor antagonist AP5 (**Fig. 6a**). These responses were duplicated by NMDA but not by agents activating other glutamate receptors, such as AMPA, t-ACPD and, notably, DHPG. Of 52 INS-1 cells challenged with DHPG, only 2 responded with rises in $[Ca^{2+}]_i$, and these were much slower and smaller than those triggered by glutamate or NMDA. Parallel experiments did not detect release of glutamate[9] from INS-1 cells stimulated with DHPG (100 μM for 2 s; $n = 4$).

We then used isolated cell pairs formed by an astrocyte with an INS-1 cell in direct lateral contact (**Fig. 6b**) and simultaneously monitored changes in acridine orange fluorescence from VGLUT+ vesicles (in the astrocyte) and fura-2 fluorescence changes (in the INS-1 cell) during 2-s pulses of DHPG, with intervening wash periods. In 17 cell pairs, DHPG always induced the same sequence of events: a burst of acridine orange flashes in the astrocyte followed by a $[Ca^{2+}]_i$ elevation in the INS-1 cell (**Fig. 6b**). The two responses were correlated, with an average delay of 599 ± 171 ms between the flash peak and the calcium peak. Both returned to baseline during the wash and reappeared, with the same sequential order and time interval, when DHPG was applied again. Moreover, if the second pulse of DHPG evoked fewer acridine orange flashes than the first pulse (**Fig. 6b**), the $[Ca^{2+}]_i$ rise in the INS-1 cell was smaller ($n = 3$ cell pairs). Therefore, the two responses must be correlated and sustained by a defined sequence of signaling events. The $[Ca^{2+}]_i$ elevation in the INS-1 cell is glutamate dependent, because in the presence of the NMDA antagonist AP5, application of DHPG induced almost no $[Ca^{2+}]_i$ rise in the INS-1 cell (although it evoked the usual pattern of acridine orange flashes in the astrocyte; **Fig. 6c**). Upon washout of AP5, however, the same INS-1 cell responded to DHPG with a large $[Ca^{2+}]_i$ rise that correlated with the acridine orange flashes (the Ca^{2+} response with AP5 was 22 ± 5% of that obtained after its washout). When cells were pre-incubated with TeNT, DHPG elicited neither acridine orange flashes in the astrocyte nor $[Ca^{2+}]_i$ increase in the INS-1 cell (**Fig. 6d**), although it enhanced $[Ca^{2+}]_i$ in the astrocyte (ΔR 340/380: 0.30 ± 0.04; $n = 4$). Taken together, these data confirm that acridine orange flashes monitor exocytosis of glutamate-containing vesicles. Astrocytes do not acquire competence to exocytose glutamate because of the induced expression of VGLUT-EGFP. Thus, nontransfected cells also responded to DHPG stimulation with acridine orange flashes accompanied by correlated Ca^{2+} responses in INS-1 cells (flash peak to calcium peak = 680 ± 56 ms), and the Ca^{2+} responses were blocked by AP5 (–75 ± 9%; $n = 6$ cell pairs).

DISCUSSION

Properties and distribution of the astrocytic microvesicles

The small vesicles identified in hippocampal astrocytes share morphological and molecular properties with synaptic vesicles of glutamatergic nerve terminals, notably their size (~30 nm in diameter), rounded shape, clear appearance and expression of VGLUT and v-SNARE proteins. The astrocytic vesicles, however, expressed cellubrevin rather than VAMP2, the main v-SNARE isoform of synaptic vesicles. Whether this molecular difference imparts specific properties to the fusion process in astrocytes remains to be established. Other aspects, particularly concerning distribution, distinguish astrocytic vesicles from synaptic ones. Astrocytic vesicles often were in smaller and less-ordered groups than synaptic vesicles. In keeping with this, lower levels of VGLUT1 and VGLUT2 were found in the astrocyte processes than were in the surrounding nerve terminals. This can explain why initial studies did not detect glial labeling[31], as it

is difficult to discern in the background of strong neuronal labeling. We succeeded by specifically marking the astrocytic processes and by comparing VGLUT immunoreactivity in the processes with the level of background labeling. The less-dense packing of the astrocytic VGLUT-containing vesicles as compared with synaptic vesicles could be another reason why the astrocytic vesicles were previously unrecognized on electron micrographs. This different arrangement might reflect a different organization of the astrocytic vesicles in the cytoplasm, for example, in their interactions with the cytoskeleton.

Single-cell PCR and immunolabeling results indicate that neither VGLUT1 or 2 is present in all of the astrocytes in the dentate gyrus, and both provide a roughly similar estimate of the number of positive cells (25–40%). It is therefore possible that VGLUT-positive vesicles are present only in subpopulations of astrocytes, which would identify a new type of heterogeneity of these cells[32]. Alternatively, astrocytes that are negative for VGLUT1 and 2 could express the VGLUT3 isoform[33], which we did not study. Diversity is found also at the ultrastructural level. VGLUT-carrying vesicles were not observed in all of the astrocytic processes, and they were not uniformly present in the processes that were positive, which indicates that they may be located at distinct sites. We often found these VGLUT-carrying vesicles just beneath the astrocytic plasma membrane that was in opposition to neuronal structures, either nerve terminals or dendrites, that expressed glutamate receptors (notably of the NMDA type); it is of note that the distance between the astrocytic membranes and the neuronal structures was similar to that at synapses (**Fig. 2c**). Such groups of VGLUT-containing vesicles could, therefore, represent sites for point-to-point transmission from astrocytes to neurons.

Properties of glutamate exocytosis from astrocytes

Exocytosis of VGLUT-expressing vesicles was studied in cultured astrocytes, where we identified a vesicle population that is structurally and biochemically homologous to VGLUT-expressing vesicles of tissue astrocytes. TIRF microscopy in combination with two fluorophores, acridine orange and VGLUT-EGFP, enabled us to monitor exocytosis of individual glutamate-containing vesicles directly and to collect information on the secretory process evoked by activation of group I mGluRs. This occurred as an exocytic burst involving about one-third of the VGLUT-positive vesicles present in the TIRF field, most likely the readily releasable pool[34]. The burst lasted 500–600 ms, but most fusions occurred within the first 200 ms. These kinetics provide a temporal frame to the stimulus–secretion coupling mechanism of astrocytes, which seems to be a most rapid process—perhaps the most rapid process—activated by G protein receptor–dependent Ca^{2+} release from internal stores[35]. Rapid fusion occurs in pituitary gonadotrophs stimulated with either gonadotropin-releasing hormone or inositol trisphosphate, its intracellular messenger[36]. The rapid coupling was ascribed to a local release of Ca^{2+} from internal stores near the exocytic sites[36]. Such a local control could be operating also in the astrocytes, because as in gonadotrophs[36], the Ca^{2+}-dependent exocytic burst largely precedes the cell-averaged $[Ca^{2+}]_i$ elevation (the latter peaks 1.4 s after the start of DHPG application; data not shown). Also, tubular structures resembling smooth endoplasmic reticulum are present in the thin processes of tissue astrocytes. For example, the structure identified in **Figure 1e** is just 50–150 nm away from both VGLUT1-positive vesicles and the plasmalemma. Whether glutamate secretion is indeed controlled by localized Ca^{2+} elevations near the plasma membrane that are dependent on smooth endoplasmic reticulum remains to be established by future studies that will require techniques with high spatial and temporal resolution[37].

Dual labeling of the vesicles with a marker of the lumen (acridine orange) and a marker of the membrane (VGLUT-EGFP) provided information on the modalities of vesicle fusion. Whereas acridine orange images marked the moment of fusion for a given vesicle, EGFP images taken soon after the fusion event signaled changes in the vesicle shape as a result of fusion. Heterogeneous fusion modes[38] were observed, as some EGFP spots rapidly disappeared after exocytosis, but others persisted, unchanged in shape and fluorescence intensity. Several explanations exist for loss of EGFP fluorescence[18], but most likely it signals a complete fusion of the vesicle and plasma membranes. In contrast, persistence of the postexocytic vesicles indicates a kiss-and-run type of fusion, with release of the vesicle content through a transiently opened fusion pore[39]. Kiss-and-run fusion is associated with a rapid recycling pathway that renders the vesicles readily reusable for exocytosis[39]. This could be of importance for rapid cross-talk between neurons and glia.

Significance of glutamate exocytosis from astrocytes

Our study provides an initial framework for understanding the significance of glutamate exocytosis from astrocytes in the context of signal exchanges between glia and neurons.

In terms of kinetics, the sharp exocytic burst triggered by mGluR stimulation, although not as rapid as the process in synapses, is in the time scale of the most rapid responses of specialized secretory cells[40]. Obviously this newly identified property of astrocytes in culture awaits confirmation from studies in the intact tissue. The close localization of astrocytic VGLUT-containing vesicles with neuronal NMDA receptors in the hippocampus indicates that astrocytes *in situ* may focally secrete glutamate onto neurons. Coupled to the evidence of focal glutamate secretion from neurons to glia[41], this observation highlights an emerging specificity of neuron–glia communication. According to theoretical calculations, a single hippocampal astrocyte could oversee more than 100,000 synapses[42]. On the other hand, its contacts could be highly compartmentalized. For example, in the cerebellum, a vast number of Bergmann glial processes enwrap small groups of Purkinje cell synapses and respond independently to parallel fiber stimulation[43]. Our observation that VGLUT-carrying vesicles are distributed unevenly in the processes of hippocampal astrocytes supports the view that astrocytes exchange independent messages at different subcellular locations. Focal glutamate signals from astrocytes could serve to orchestrate subsets of synapses in functional microdomains.

In conclusion, the presented evidence that many astrocytes contain a vesicular compartment for regulated glutamate secretion strongly indicates that this may be a candidate mechanism for information processing by glia in concert with neurons and provides a concrete basis for redefinition of the roles these cells play in brain function.

METHODS

Electrophysiology and single-cell RT-PCR. Hippocampal slices were prepared from postnatal day (P) 35–70 rats, and cells in the outer molecular layer of the dentate gyrus were selected for whole-cell recordings as reported[23]. Use of animals and experimental procedures were approved by the Office Veterinaire Cantonal (Lausanne), in accordance with the Swiss Federal Laws. After electrophysiological identification, cells were isolated by lifting them out of the tissue while harvesting the cytoplasm under microscopic control[24]. Only individual cells without any adhered tissue debris were selected for RT-PCR analysis. Single-strand cDNA synthesis and multiplex two-round single-cell PCR was as described[32], with primers for VGLUT1, VGLUT2 and S100β (for sequences, see **Supplementary Table 1**). Primer pairs were located on different exons to prevent amplification of genomic DNA. Omission of reverse transcriptase and aspiration of bath solution served as negative controls.

Antibodies. Rabbit VGLUT1 and VGLUT2 antibodies to peptide sequences containing the carboxy-terminal 68 (VGLUT1) and 64 amino acids (VGLUT2; both gifts from R. Edwards, University of California at San Francisco School of Medicine), which are highly specific[31,44], were diluted 1:100 and 1:2,000 (respectively, for immunogold labeling) and 1:1,000 (for both, for immunofluorescence). A mixture of rabbit antibodies to GLT and GLAST[25] (both gifts from N.C. Danbolt, Anatomical Institute, University of Oslo) was used at a final dilution of 1 μg/ml. Rabbit antibodies to cellubrevin[45] (gift from P. De Camilli, Yale University School of Medicine) were diluted 1:1,500 (immunoflourescence) and 1:100 (immunogold). A mixture of antibodies to the NMDA receptor subunits 1 and 2A/B (final dilution 1:50) and a monoclonal antibody to GFAP (diluted 1:1,000) were from Chemicon. A monoclonal antibody to VAMP2 (Synaptic Systems) was diluted 1:500 (immunofluorescence) and 1:100 (immunogold). Antibodies to EGFP (BD Biosciences) were diluted 1:100.

Immunocytochemistry. Immunogold cytochemistry was carried out as described[24,46] using hippocampal specimens from adult Wistar rats fixed by perfusion through the heart (4% formaldehyde and 0.1% glutaraldehyde) and rat primary astrocyte cultures (see below), with the same fixative. These tissues were embedded at low temperature in Lowicryl HM20 or K4M. Ultrathin sections were treated with the antibodies and were viewed in a Philips CM 100 electron microscope. Electron micrographs were taken in the superficial granule cell layer and in the molecular layer of the dentate gyrus. Astrocytic processes were identified by the presence of filaments and/or by labeling for GLT/GLAST[25]. The densities of gold particles signaling the presence of VGLUT1 and VGLUT2 were quantified as before[46]. Only VGLUT1 or 2 signals that were twice the amount of background labeling seen over mitochondria were included in the quantifications. The spatial relationship between gold particles signaling VGLUT1 or VGLUT2 (10 nm) and cellubrevin or VAMP2 (15 nm) were determined by digitizing the positions of their centers with the program MicroTrace[47] and then calculating the intercenter distances between the 10- and 15-nm gold particles with custom software (mitochondria and areas apparently lacking electron-dense material were excluded). The distances were sorted into bins of 20 nm. The distributions were compared with those of random points to gold particle centers[47]. With the exception of the excluded regions described above, 1,000 random points were spread over the astrocyte.

Pre-embedding electron microscopy was done on cultured astrocytes that were transfected with a construct to express cellubrevin-EGFP[26] (gift from T. Coppola and R. Regazzi, Department of Cell Biology and Morphology, University of Lausanne), fixed as above and peroxidase-labeled according to a biotin–streptavidin method[46] before embedding in Durcupan ACM.

Immunofluorescence was carried out as described[11] on cultured astrocytes transfected with either cellubrevin-EGFP or VGLUT2-EGFP constructs or on intact hippocampal tissue. Primary antibodies were visualized with Cy3-conjugated secondary antibodies (Jackson ImmunoResearch Laboratories) and viewed on a Zeiss Axioplan 2 microscope. Colocalization analysis in cultured cells was done on fluorescent spots representing individual vesicles. The average diameter of a single vesicle was calculated indirectly from TIRF images where a single flash represented a single fusion event (**Fig. 3**). Only spots overlapping by ≥66% were considered to be colocalized.

Preparation and transfection of VGLUT-EGFP. To fuse rat genes encoding VGLUT1 and VGLUT2 in pcDNA3 mammalian expression plasmids (gifts of R. Edwards) with a vector containing the EGFP coding sequence, restriction sites *Eco*RI and *Xho*I were generated by PCR. The PCR products (1,698 base pairs for VGLUT1 and 1,764 bp for VGLUT2) were purified (Microcon-PCR, Millipore) and subcloned into the EGFP vector (Clontech) at the *Eco*RI–*Xho*I site under the control of the CMV promoter. Restriction analysis, sequencing (Microsynth) and western blots indicated the successful construction of the fusion proteins. Either VGLUT1-EGFP or VGLUT2-EGFP plasmid (1 μg) was transfected into primary cultures of rat cortical astrocytes with Fugene6 transfection reagent (Roche). In most experiments, we used VGLUT2-EGFP because of its higher transfection yield.

Astrocyte and INS-1 cell cultures for imaging experiments. Cultures of pure astrocytes (>99% GFAP positive), prepared as described[11], were plated (2.5×10^4 cells) on glass coverslips and used 2–3 d after transfection with the VGLUT-EGFP construct. INS-1 insulinoma cells were plated either alone (1.5×10^5 cells) or on the transfected astrocytes and used the next day. For acridine orange imaging experiments, cells were stained with 5 μM acridine orange (Molecular Probes) for 15 min at 34 °C in the dark. For single-cell $[Ca^{2+}]_i$ measurements, cells were loaded with 5 μM fura-2 AM and 0.02% pluronic acid (both from Molecular Probes) for 30 min. For combined acridine orange and fura-2 imaging, fura-2 loading was followed by 15 min of staining with acridine orange. Coverslips were mounted in an open perfusion micro-incubator at 37 °C (PDMI-2, Harvard Apparatus). Stimuli (DHPG, glutamate, NMDA, AMPA and t-ACPD from Tocris Cookson Ltd.; ionomycin and α-latrotoxin from Fluka) were applied onto cells by a local microperfusion system driven by electrovalves (Warner Instrument Corporation).

Optical imaging. A Zeiss Axiovert 200 inverted fluorescence microscope was modified to allow both epifluorescence and evanescent field (EF) illumination (Visitron Systems). For EF illumination, the expanded beam (488-nm argon ion laser, 40 mW; Laserphysics) was passed through a shutter driver (Uniblitz, VMM-D1 model, Vincent Associates) that was synchronized with a SNAP-HQ CCD camera (Roper Scientific) under Metafluor software (Universal Imaging) control and introduced from the high numerical aperture objective lens (Zeiss α-plan FLUAR 100×, 1.45 n.a.). Light entered the coverslip at an angle of 72.3–73.8° and underwent total internal reflection at the glass–cell interface. The refractive indices for glass ($n = 1.52$ at 488 nm) and cells ($n = 1.38$) predict an EF declining *e*-fold within 84 nm from the interface.

We imaged EGFP and acridine orange fluorescence simultaneously under EF illumination as described[18]. The images, projected side by side, were acquired at either 10 or 20 interlaced frames/s. To image both fura-2 and acridine orange fluorescence, we combined EF (488 nm laser) and epifluorescence illumination (340/380-nm xenon arc lamp, Visichrome polychromator system, Visitron). Lights were filtered with a beam splitter (Zeiss filter set 25). Images were further separated using a filter wheel optical system (Lambda-10A, Sutter) equipped with two Zeiss emission filters (bandpass 515–565 nm for acridine orange and bandpass 505–530 nm for fura-2). They were then acquired at 10 interlaced frames/s and projected side by side.

Image analysis. Video images, digitized with MetaFluor, were analyzed with MetaMorph software (Universal Imaging). Movements of VGLUT-positive acridine orange spots in unstimulated astrocytes were measured by positioning a circle (diameter, 895 nm) on the spot at the beginning of the experiment, taking the distance from the center of this circle at each frame and averaging it per second. Acridine orange flashes were measured (in red images) as fluorescence intensity changes (arbitrary units, a.u.) in a circle as above, and in a concentric annulus (895-nm inner and 1,195-nm outer diameter)[20]. Only when fluorescence increased, spread and then declined, was the event counted as a flash[20]. The fate of VGLUT-EGFP spots (in green images) was analyzed by positioning a circle as above on each spot and by comparing fluorescence intensity just before stimulating the cell (with DHPG) and 300 ms after an acridine orange flash was observed in the red images. Changes in fura-2 fluorescence were measured with the 340/380-nm excitation wavelength ratio method (R340/380) in a circle centered on the cell soma.

Note: Supplementary information is available on the Nature Neuroscience website.

ACKNOWLEDGMENTS

We thank H. Stubbe, Y. Gomez, K. Hüttmann and Centre de Microscopie Electronique, University of Lausanne for experimental support; J.-Y. Chatton, T. Coppola, P. Jourdain, G. Knott, T. Lang and R. Stoop for scientific discussions; R. Jahn, J. Storm-Mathisen for insights at various stages of this work and P. Clarke, J. Meldolesi, R. Regazzi and J. Storm-Mathisen for comments on the manuscript. This work was supported by grants OFES 00.0553 and FNRS 3100A0-100850/1 to A.V. and by Deutsche Forschungsgemeinschaft (SFB-TR3) and Fonds der Chemischen Industrie to C.S. V.G. is a visiting fellow within the European Community grant QLG3-CT-2001–2004 and recipient of a fellowship from the Norwegian Research Council.

COMPETING INTERESTS STATEMENT

The authors declare that they have no competing financial interests.

Received 5 February; accepted 5 April 2004
Published online at http://www.nature.com/natureneuroscience/

1. Volterra, A. & Bezzi, P. Release of transmitters from glial cells. in *The Tripartite Synapse: Glia in Synaptic Transmission* (eds. Volterra, A., Magistretti, P.J. & Haydon, P.G.) 164–182 (Oxford Univ. Press, Oxford, UK, 2002).
2. Parri, R.H., Gould, T.M. & Crunelli, V. Spontaneous astrocytic Ca^{2+} oscillations *in situ* drive NMDAR-mediated neuronal excitation. *Nat. Neurosci.* **4**, 803–812 (2001).
3. Pasti, L., Volterra, A., Pozzan, T. & Carmignoto, G. Intracellular calcium oscillations in astrocytes: a highly plastic, bidirectional form of communication between neurons and astrocytes *in situ*. *J. Neurosci.* **17**, 7817–7830 (1997).
4. Kang, J., Jiang, L., Goldman, S.A. & Nedergaard, M. Astrocyte-mediated potentiation of inhibitory synaptic transmission. *Nat. Neurosci.* **1**, 683–692 (1998).
5. Zhang, J.M. *et al.* ATP released by astrocytes mediates glutamatergic activity-dependent heterosynaptic suppression. *Neuron* **40**, 971–982 (2003).
6. Newman, E.A. Propagation of intercellular calcium waves in retinal astrocytes and Müller cells. *J. Neurosci.* **21,** 2215–2223 (2001).
7. Schipke, C.G., Boucsein, C., Ohlemeyer, C., Kirchhoff, F. & Kettenmann, H. Astrocyte Ca^{2+} waves trigger responses in microglial cells in brain slices. *FASEB J.* **16**, 255–257 (2002).
8. Parpura, V. *et al.* Glutamate-mediated astrocyte-neuron signalling. *Nature* **369**, 744–747 (1994).
9. Bezzi, P. *et al.* Prostaglandins stimulate calcium-dependent glutamate release in astrocytes. *Nature* **391**, 281–285 (1998).
10. Newman, E.A. New roles for astrocytes: regulation of synaptic transmission. *Trends Neurosci.* **26**, 536–542 (2003).
11. Bezzi, P., *et al.* CXCR4-activated astrocyte glutamate release via TNFα: amplification by microglia triggers neurotoxicity. *Nat. Neurosci.* **4**, 702–710 (2001).
12. Araque, A., Li, N., Doyle, R.T. & Haydon, P.G. SNARE protein-dependent glutamate release from astrocytes. *J. Neurosci.* **20**, 666–673 (2000).
13. Pasti, L., Zonta, M., Pozzan, T., Vicini, S. & Carmignoto G. Cytosolic calcium oscillations in astrocytes may regulate exocytotic release of glutamate. *J. Neurosci.* **21**, 477–484 (2001).
14. Volterra, A. & Meldolesi, J. Quantal release of transmitter: not only from neurons but from astrocytes as well? in *Neuroglia,* Edn. 2 (eds. Kettenmann, H. & Ransom, B.) 190–201 (Oxford Univ. Press, New York, 2004).
15. Nedergaard, M., Takano, T. & Hansen, A.J. Beyond the role of glutamate as a neurotransmitter. *Nat. Rev. Neurosci.* **3**, 748–754 (2002).
16. Fremeau, R.T. Jr., Voglmaier, S., Seal, R & Edwards, R.H. VGLUTs define subsets of excitatory neurons and suggest novel roles for glutamate. *Trends Neurosci.* **27**, 98–103 (2004).
17. Jahn, R., Lang, T. & Südhof, T.C. Membrane fusion. *Cell* **112**, 519–533 (2003).
18. Tsuboi, T., Zhao, C., Terakawa, S. & Rutter, G.A. Simultaneous evanescent wave imaging of insulin vesicle membrane and cargo during a single exocytotic event. *Current Biol.* **10**, 1307–1310 (2000).
19. Avery, J. *et al.* A cell-free system for regulated exocytosis in PC12 cells. *J. Cell. Biol.* **148**, 317–324 (2000).
20. Zenisek, D., Steyer, J.A. & Almers, W. Transport, capture and exocytosis of single synaptic vesicles at active zones. *Nature* **406**, 849–854 (2000).
21. Stout, A.L. & Axelrod, D. Evanescent field excitation of fluorescence by epiillumination microscopy. *Appl. Optics* **28**, 5237–5242 (1989).
22. Steyer, J.A. & Almers, W. A real-time view of life within 100 nm of the plasma membrane. *Nat. Rev. Mol. Cell. Biol.* **2**, 268–275 (2001).
23. Schröder, W. *et al.* Lesion-induced changes of electrophysiological properties in astrocytes of the rat dentate gyrus. *Glia* **28**,166–174 (1999).
24. Seifert, G., Becker, A. & Steinhäuser, C. Combining patch-clamp techniques with RT-PCR in *Neuromethods: Patch-clamp Analysis: Advanced Techniques* Vol 35 (eds. Walz, W., Boulton, A.A. & Baker, G.B.) 301–330 (Humana Press, Totowa, NJ, 2002).
25. Chaudhry, F.A. *et al.* Glutamate transporters in glial plasma membranes: highly differentiated localizations revealed by quantitative ultrastructural immunocytochemistry. *Neuron* **15**, 711–720 (1995).
26. Randhawa, V.K. *et al.* VAMP2, but not VAMP3/cellubrevin, mediates insulin-dependent incorporation of GLUT4 into the plasma membrane of L6 myoblasts. *Mol. Biol. Cell.* **11**, 2403–2417 (2000).
27. Steyer, J.A., Horstmann, H. & Almers, W. Transport, docking and exocytosis of single secretory granules in live chromaffin cells. *Nature* **388**, 474–478 (1997).
28. Rosenthal, L. & Meldolesi, J. Alpha-latrotoxin and related toxins. *Pharmacol. Ther.* **42**, 115–134 (1989).
29. Muyderman, H. *et al.* α_1-adrenergic modulation of metabotropic glutamate-receptor induced calcium oscillations and glutamate release in astrocytes. *J. Biol. Chem* **276**, 46504–46514 (2001).
30. Humeau, Y., Doussau, F., Grant, N.J. & Poulain, B. How botulinum and tetanus neurotoxins block neurotransmitter release. *Biochimie* **82**, 427–446 (2000).
31. Fremeau, R.T. Jr. *et al.* The expression of vesicular glutamate transporters defines two classes of excitatory synapse. *Neuron* **31**, 247–260 (2001).
32. Matthias, K. *et al.* Segregated expression of AMPA-type glutamate receptors and glutamate transporters defines distinct astrocyte populations in the mouse hippocampus. *J. Neurosci.* **23**, 1750–1758 (2003).
33. Fremeau, R.T. Jr. *et al.* The identification of vesicular glutamate transporter 3 suggests novel modes of signaling by glutamate. *Proc. Natl. Acad. Sci. USA* **99**, 14488–14493 (2002).
34. Xu, T., Binz, T., Niemann, H. & Neher, E. Multiple kinetic components of exocytosis distinguished by neurotoxin sensitivity. *Nat. Neurosci.* **1**, 192–200 (1998).
35. Tse, F.W. & Tse, A. Regulation of exocytosis via release of Ca^{2+} from intracellular stores. *Bioessays* **21**, 861–865 (1999).
36. Tse, F.W., Tse, A., Hille, B., Horstmann, H. & Almers, W. Local Ca^{2+} release from internal stores controls exocytosis in pituitary gonadotrophs. *Neuron* **18**, 121–132 (1997).
37. Becherer, U., Moser, T., Stümer, W. & Oheim, M. Calcium regulates exocytosis at the level of single vesicles. *Nat. Neurosci.* **8**, 846–853 (2003).
38. Alés, E. *et al.* High calcium concentrations shift the mode of exocytosis to the kiss-and-run mechanism. *Nat. Cell. Biol.* **1**, 40–44 (1999).
39. Valtorta, F., Meldolesi, J. & Fesce, R. Synaptic vesicles: is kissing a matter of competence? *Trends Cell. Biol.* **11**, 324–328 (2001).
40. Kasai, H. Comparative biology of Ca^{2+}-dependent exocytosis: implications of kinetic diversity for secretory function. *Trends Neurosci.* **22**, 88–93 (1999).
41. Matsui, K. & Jahr, C.E. Ectopic release of synaptic vesicles. *Neuron* **40**, 1173–1183 (2003).
42. Bushong, E.A., Martone, M.E., Jones, Y.Z. & Ellisman, M.H. Protoplasmic astrocytes in CA1 stratum radiatum occupy separate anatomical domains. *J. Neurosci.* **22**, 183–192 (2002).
43. Grosche, J. *et al.* Microdomains for neuron-glia interaction: parallel fiber signalling to Bergmann glial cells. *Nat. Neurosci.* **2**, 139–143 (1999).
44. Bellocchio, E.E. *et al.* The localization of the brain-specific inorganic phosphate transporter suggests a specific presynaptic role in glutamatergic transmission. *J. Neurosci.* **18**, 8648–8659 (1998).
45. Chilcote, T.J. *et al.* Cellubrevin and synaptobrevins: similar subcellular localization and biochemical properties in PC12 cells. *J. Cell. Biol.* **129**, 219–231 (1995).
46. Gundersen, V. *et al.* Synaptic vesicular localization and exocytosis of L-aspartate in excitatory nerve terminals: a quantitative immunogold analysis in rat hippocampus. *J. Neurosci.* **18**, 6059–6070 (1998).
47. Bergersen, L., Ruiz, A., Bjaalie, J.G., Kullmann, D.M. & Gundersen, V. GABA and GABAA receptors at hippocampal mossy fibre synapses. *Eur. J. Neurosci.* **18,** 931–941 (2003).